

ANDRZEJ J. OSIADACZ^{*1}, FERDINAND E. UILHOORN*, MACIEJ CHACZYKOWSKI*

NON-LINEAR OPTIMIZATION OF HIGH-PRESSURE GAS NETWORKS WITH RESPECT TO HYDRATE CONTROL

NIELINIOWA OPTYMALIZACJA SIECI GAZOWEJ WYSOKIEGO CIŚNIENIA Z UWZGLĘDNIENIEM ZAPOBIEGANIU HYDRATÓW

In this paper, gas pipeline optimization includes constraints resulting from hydrate prevention. The key is to seek for the optimal settings of both: the compressor units and hydrate combating method at minimum fuel consumption subject to security of supply and hydrate prevention. A case study is conducted on the Polish section of the Yamal pipeline and an arbitrarily selected partial onshore and offshore pipeline. Three different configurations are investigated: (i) cooling the compressed gas, (ii) no cooling and (iii) line heating immediately after the compressor station. For each configuration, the fuel consumption of the compressors is minimized and in order to prevent hydrate formation, the outlet temperature of the line heater, allowable water vapour in the gas and methanol concentration are calculated for each pipe section. The hydrate model is based on the statistical mechanical approach of Van der Waals and Platteeuw and applicable for systems that contain water (free or dissolved in gas), methanol and mixed gases both hydrate and non-hydrate formers.

Keywords: Phase Equilibria; Gas hydrates; Mathematical modelling; Thermodynamics; Optimization

W artykule omówiono zagadnienie optymalizacji gazowego systemu przesyłowego uwzględniając dodatkowo ograniczenia wynikające z warunków tworzenia się hydratów. Kryterium optymalizacji to minimum zużycia paliwa w tłoczniach gazu. Badania przeprowadzono na polskiej części gazociągu jamalskiego dla trzech przypadków pracy tłoczni: chłodzenie gazu w tłoczni, brak chłodzenia oraz podgrzewanie gazu za stacją przetłoczną. Dla każdego wariantu, zużycie paliwa przez sprężarki jest minimalizowane oraz w celu przeciwdziałania tworzenia się hydratów, temperatura wyjściowa podgrzewacza jest obliczana a także obliczana jest zawartość pary wodnej i metanolu w gazie dla każdej sekcji gazociągu. Zastosowany model hydratu jest oparty na modelu Van der Waalsa oraz Platteeuw.

Słowa kluczowe: hydraty gazowe, modelowanie matematyczne, termodynamika, optymalizacja, równowagi fazowe

* HEATING AND GAS ENGINEERING DIVISION, FACULTY OF ENVIRONMENTAL ENGINEERING, WARSAW UNIVERSITY OF TECHNOLOGY, UL. NOWOWIEJSKA 20, 00-653 WARSZAWA, POLAND

¹ Corresponding Author. TEL.: +4822 660 53 11. FAX.: +48 22 825 29 92, E-mail: andrzej.osiadacz@is.pw.edu.pl

Nomenclature

- a – Radius spherical core, Å
 $c_1, c_2, c_3, c_4, c_5, c_5$ – Coefficients to define polytropic head and efficiency, -;
 $C_{k,m}$ – Langmuir constant of molecule k in cavity m , Pa⁻¹;
 c_p – Specific heat capacity at constant pressure, J/(kg · K);
 d – Pipe diameter, m;
 d_o – Outside pipe diameter, m;
 f – Friction factor, -, fugacity, Pa;
 H – Specific enthalpy, J/mol;
 $H_{i,w}$ – Henry's constants of component i in water, Pa⁻¹;
 H_i – Net caloric value, MJ/kg;
 H_p – Polytropic head, m · kgf/kg · m;
 \bar{h}_c – Average heat transfer convection coefficient, W/(m² · K);
 k – Thermal conductivity, W/(m · K), Boltzmann constant, J · K, isentropic coefficient, -;
 K – Average height of all protrusions in the pipe, m;
 k_{gas} – Thermal conductivity of gas, W/(m · K);
 k_{soil} – Thermal conductivity of soil, W/(m · K);
 \dot{m} – Mass flow rate in the pipeline, kg/s;
 M – Molar mass, kg/mol;
 n – Polytropic coefficient, -;
 n_r – Compressor speed, rpm;
 \dot{n} – Fuel consumption of gas turbine, kg/s;
 p – Pressure, Pa;
 p_{in} – Inlet pressure compressor, Pa;
 p_n – Pressure at normal conditions, Pa;
 p_{out} – Outlet pressure compressor, Pa;
 q – Flowrate, m³/s;
 q_n – Gas flow at normal conditions, m³/s;
 R – Gas constant, J/(kg · K);
 Re – Reynolds number, -;
 R_m – Free radius of cavity type m , Å;
 R_{tot} – Overall thermal resistance, m · K/W;
 S – Shape factor, -;
 T – Temperature, K;
 T_∞ – Surrounding temperature, K;
 T_{in} – Inlet temperature, K;
 T_{out} – Outlet temperature compressor, K;
 V – Specific molar volume, m³/mol;
 x – Distance along the pipeline, -;
 x_{MeOH} – Mole fraction of methanol, -;
 $y_{k,m}$ – Fractional occupancy of cavity m by guest molecule k , -;
 z – Compressibility factor, -, coordination number, -, depth of the pipeline, m;
 z_n – Compressibility factor at normal conditions, -.

Greek symbols

- α – Ice phase;
- β – Empty hydrate lattice;
- ε – Depth of the potential well (J);
- η_g – Efficiency gas turbine, -;
- η_p – Polytropic efficiency, -;
- γ_i – Activity coefficient of component i ;
- μ – Dynamic viscosity, Pa · s, chemical potential of water in ice phase, J/mol;
- ν – Number of cavities per water molecule, -;
- ω – Spherically symmetrical potential energy (J);
- ρ – Density, kg/m³;
- ρ_n – Density at normal conditions, kg/m³;
- σ – Cores distance at zero potential (Å).

Phases

- H – Clathrate hydrate;
- I – Ice;
- L – Liquid.

1. Introduction

The compressor stations are important elements in the natural gas transmission system. Efficient operation and design is from vital importance to enhance the performance of the pipeline system. However, it is not common to operate the compressors at minimum fuel consumption, while maintaining the desired throughput in the line. Moreover, to minimize the cost of the hydrate combating strategy. The formation of gas hydrates must be avoided due to their proclivity to plug pipelines causing costly production stops. Each hydrate combating method contributes to the capital and operating cost, as well as the complexity of the system. Hence, besides the necessity to improve the economics of running the compressors, minimizing the cost of hydrate control is also advocated.

Mathematical optimization of gas networks is a complicated problem. The problem is time dependent as the conditions in pipelines are always in flux. However, when demand is constant over a longer period the network tends to be in stationary state. In this work, a steady-state situation is assumed and without large variations in pressure and flow, this approach is very useful. The objective is to seek for both the optimal settings of the compressor units and hydrate combating methods at minimum fuel consumption within security of supply. The hydrate prevention strategies are dehydration, line heating and methanol injection. The problem is formulated as a nonlinear programming problem. The constraints imposed on a gas pipeline system are: (i) mass flow balance equations, (ii) nonlinear momentum constraint in each pipe, (iii) energy balance equations, (iv) pressure limits at each node, (v) operational limits of each compressor and (vi) pressure and temperature limits to preclude hydrates.

2. Pipe flow equations

In a steady state situation, the momentum equation for a horizontal pipeline reduces to the following simplified expression

$$p(x) = \left(p(0)^2 - \frac{4^2 q_n^2 \rho_n p_n z T}{\pi^2 Z_n T_n} \frac{f}{d^5} x \right)^{\frac{1}{2}} \quad (1)$$

where the friction factor, f , is calculated from (Techo et al., 1965)

$$f = -0.8685 \ln \left(\frac{1.964 \ln(\text{Re}) - 3.8215}{\text{Re}} + \frac{K}{3.71d} \right)^{-2} \quad (2)$$

The temperature distribution along the pipeline is obtained from a simplified form of the energy equation,

$$T(x) = T_\infty + [T(0) - T_\infty] e^{-\frac{x}{\bar{m}c_p R_{tot}}} \quad (3)$$

where the total resistance for a buried pipeline has contributions from convection of the natural gas to the pipe wall and conduction through the pipe and soil. Hence,

$$R_{tot} = \frac{1}{\bar{h}_c \pi d_i dx} + \left(\sum_{i=1}^n \frac{\ln(d_{i+1}/d_i)}{2\pi k_i dx} \right) + \frac{1}{k_{soil} S} \quad (4)$$

For a buried pipeline at a distance z the shape factor S is defined as (Kreith & Bohn, 1993)

$$S = \frac{2\pi dx}{\cosh^{-1}(2z/d_o)} \quad (5)$$

The average convection heat transfer coefficient from the gas to the wall is calculated from

$$\bar{h}_c = 0.023 \left(\frac{4\dot{m}}{\pi d \mu} \right)^{4/5} \left(\frac{c_p \mu}{k_{gas}} \right)^{0.3} \frac{k_{gas}}{d} \quad (6)$$

3. Compressor equations

Each compressor operates within a feasible region. The compressor envelope and polytropic efficiency in terms of head, speed and inlet flow rate for the compressors installed along the Yamal pipeline are depicted in Figure 1 and 2, respectively. The compressor map and polytropic efficiency can both be modelled as quadratic polynomials in the following manner

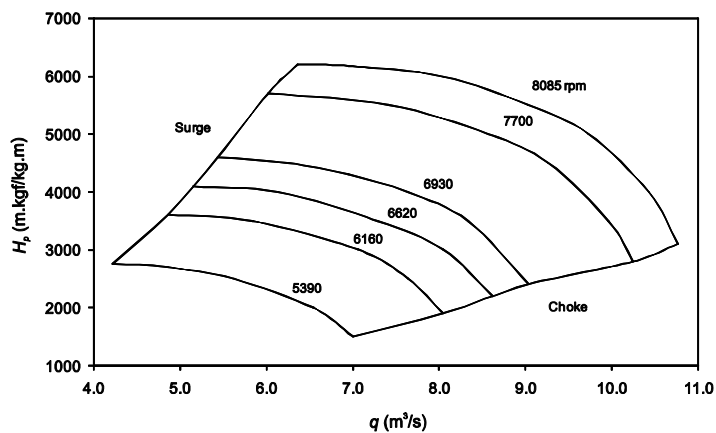


Fig. 1. Compressor envelope

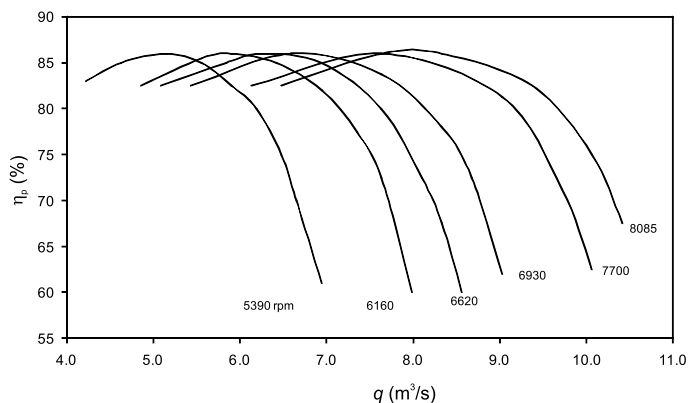


Fig. 2. Polytropic efficiency

$$H_p/n_r^2 = c_1 + c_2 q/n_r + c_3 (q/n_r)^2 \quad (7)$$

and

$$\eta_p = c_4 + c_5 q/n_r + c_6 (q/n_r)^2 \quad (8)$$

The head is defined as

$$H_p = \frac{zRT_{in}}{M} \frac{n}{n-1} \left[\left(\frac{p_{out}}{p_{in}} \right)^{\frac{n-1}{n}} - 1 \right] \quad (9)$$

The required power from the prime mover is $N_p = (\rho_n Q_n / \eta_t) H_p$ where $\eta_t = \eta_m \eta_p$. The polytropic exponent n ($n \neq 1$) is

$$\frac{n}{n-1} = \left(\frac{k}{k-1} \right) \eta_p \quad (10)$$

and the isentropic exponent k is given by

$$k = \frac{z}{z - p \left(\frac{\partial z}{\partial p} \right)_T - \frac{Rz}{c_p} \left[1 + \frac{T}{z} \left(\frac{\partial z}{\partial T} \right)_p \right]^2} \quad (11)$$

The outlet temperature of the compressor is

$$\frac{T_{out}}{T_{in}} = \left(\frac{P_{out}}{P_{in}} \right)^{\frac{n-1}{n}} \quad (12)$$

The fuel consumption of the gas turbine is calculated from $\dot{n} = N_p / H_i \eta_g$ where H_i is the net caloric value and η_g the turbine efficiency. The latter is given in Eq. 32.

4. Hydrate model

By means of statistical mechanics Van der Waals and Platteeuw (1959) derived from the partition function the chemical potential of water in the hydrate phase, yielding

$$\Delta \mu_w^{(\beta-H)} = \mu_w^{(\beta)} - \mu_w^{(H)} = -RT \sum_m v_m \ln \left(1 - \sum_k y_{k,m} \right) \quad (13)$$

Instead of using chemical potential as equilibrium criteria between coexisting phases, the fugacity is deployed. The equilibrium condition in fugacity format is $f_w^{(H)} = f_w^{(L \text{ or } \alpha)}$. The fugacity of water in the hydrate phase is defined as

$$f_w^{(H)} = f_w^{(\beta)} e^{\sum_m v_m \ln \left(1 - \sum_k y_{k,m} \right)} \quad (14)$$

where $f_w^{(\beta)}$ is the fugacity of the empty hydrate lattice and $y_{k,m}$ the fractional occupancy. The latter is the product of Langmuir constant and fugacity, expressed as

$$y_{k,m} = \frac{C_{k,m} f_k}{1 + \sum_i C_{i,m} f_i} \quad (15)$$

The Langmuir constant accounts for the gas-water interactions in the cavities and is defined as

$$C_{k,m} \equiv \frac{4\pi}{kT} \int_0^{R_m} e^{-\frac{\omega_{i,m}(r)}{kT}} r^2 dr \quad (16)$$

It is directly related to the configurational partition function, which depends on the intermolecular potential and integral over the interaction volume. The spherical cell potential $\omega_{i,m}(r)$ of component i in cavity m is obtained from

$$\omega_{i,m}(r) = 2z_m \varepsilon_i \left[\frac{\sigma_i^{12}}{R_m^{11} r} \left(\delta_{i,m}^{10} + \frac{a_i}{R_m} \delta_{i,m}^{11} \right) - \frac{\sigma_i^6}{R_m^5 r} \left(\delta_{i,m}^4 + \frac{a_i}{R_m} \delta_{i,m}^5 \right) \right] \quad (17)$$

and

$$\delta_{i,m}^N = \frac{1}{N} \left[\left(1 - \frac{r}{R_m} - \frac{a_i}{R_m} \right)^{-N} - \left(1 + \frac{r}{R_m} - \frac{a_i}{R_m} \right)^{-N} \right] \quad (18)$$

where R_m is the cell radius of cavity m and z the co-ordination number of the cavity. N is 4, 5, 10 or 11. The Kihara parameters are denoted as σ_i , ε_i and a_i of component i and fitted from experimental data and listed in Table 1. The chemical potential of liquid water and ice in fugacity format is

$$f_w^{(L)} = f_w^{(\beta)} e^{\left[\frac{\mu_w^{(\beta,\beta)} - \mu_w^{(L,0)}}{RT_0} \right] - \int_{T_0}^T \left[\frac{H^{(\beta)} - H^{(L)}}{RT^2} \right] dT + \int_{p_0}^p \left[\frac{V^{(\beta)} - V^{(L)}}{RT} \right] dp - \ln(x_w \gamma_w)} \quad (19)$$

and for pure ice

$$f_w^{(\alpha)} = f_w^{(\beta)} e^{\left[\frac{\mu_w^{(\beta,\beta)} - \mu_w^{(\alpha,0)}}{RT_0} \right] - \int_{T_0}^T \left[\frac{H^{(\beta)} - H^{(\alpha)}}{RT^2} \right] dT + \int_{p_0}^p \left[\frac{V^{(\beta)} - V^{(\alpha)}}{RT} \right] dp} \quad (20)$$

TABLE 1

Kihara parameters

Component	a (Å)	σ (Å)	ε/k (K)
CH ₄	0.3835	3.1713	153.9830
C ₂ H ₆	0.5654	3.3510	180.8067
C ₃ H ₈	0.6643	3.5341	184.0601
<i>i</i> -C ₄ H ₁₀	0.8073	3.5154	195.2380
<i>n</i> -C ₄ H ₁₀	0.9900	3.3166	187.9311
<i>i</i> -C ₅ H ₁₂	0.9672	3.2729	323.5897
H ₂ S	0.2025	3.3180	199.2553
N ₂	0.3545	3.1302	123.4874
CO ₂	0.8987	2.7848	171.3319

The activity coefficient is calculated from the UNIFAC model (Hansen et al., 1991). The composition of the guest molecule in the liquid phase is obtained from Henry's law, $x_{i,w} = f_{i,g}/H_{i,w}$ where $f_{i,g}$ is the fugacity of the gas component i and x_i is the mole fraction of the gas dissolved in water. The effect of pressure on Henry's constant $H_{i,w}$ is given by Krichevsky-Kasarnovsky (1935). The enthalpy difference is given by

$$\Delta H_w^{(\beta-L \text{ or } \alpha)} = H_w^{(\beta)} - H_w^{(L \text{ or } \alpha)} = \Delta H^{(\beta-L)}(T_0, p_0) + \int_{T_0}^T \Delta C_p^{(\beta-L \text{ or } \alpha)} dT \quad (21)$$

and

$$\Delta C_p^{(\beta-L \text{ or } \alpha)} = \Delta C_p^{(\beta-L \text{ or } \alpha)}(T_0) + \Delta b^{(\beta-L \text{ or } \alpha)}(T - T_0) \quad (22)$$

where $\Delta b^{(\beta-L \text{ or } \alpha)}$ is an empirical constant and

$$\Delta H^{(\beta-L)}(T_0, p_0) = \Delta H^{(\beta-\alpha)}(T_0, p_0) + \Delta H^{(\alpha-L)}(T_0, p_0) \quad (23)$$

with $\Delta H^{(\alpha-L)}(T_0)$ as the latent heat of converting water into ice. The lattice and reference properties are listed in Table 2. The molar volume of ice, liquid water and empty hydrate for sI and sII is given by (Klauda & Sandler, 2000; Yoon & Yoshitaka, 2004). The volume difference for sH is

$$\Delta V_{w,sH}^{(\beta-\alpha)} = 3.85 \times 10^6 \text{ m}^3/\text{mol} \text{ and } \Delta V_{w,sH}^{(\alpha-L)} = 1.598 \times 10^6 \text{ m}^3/\text{mol} \text{ (Sloan Jr., 1998). Now equating,}$$

$f_w^{(H)} = f_w^{(L \text{ or } \alpha)}$ and by iteration, the hydrate formation pressure or temperature for a given gas composition is calculated. A multiphase flash calculation is performed to calculate the phase of the mixture of known total composition. The predictive Soave-Redlich-Kwong (PSRK) group contribution method (Holderbaum & Gmehling, 1991) calculates the fugacity of all components in vapour and liquid phases. This method uses the Soave-Redlich-Kwong (SRK) equation of state (Soave, 1972) incorporated with the modified Huron-Vidal first-order mixing rule. The activity coefficient γ_i and g_0^E are calculated from the UNIFAC model. The procedure above assumes free water is present. In case of two-phase equilibria the algorithm is slightly modified whereas the hydrate pressure or temperature is calculated by equating, $f_w^{(H)} = f_{w,g}^L$, where $f_{w,g}^L$ is the fugacity of water in the hydrocarbon calculated with the PSRK method.

The fugacity of the empty hydrate, $f_w^{(\beta)}$ is obtained from the correlation

$$\ln(f_w^{(\beta)}) = \sum_{i=0}^{a_n} a_i p^{I_{i,0}} T^{I_{i,1}} \quad (24)$$

where I gives the power of pressure of each monomial corresponding to the power of temperature term given in the second column. The coefficients are listed in Table 3 and only valid for H-V equilibria and sI and sII hydrates. The depression of the hydrate forming temperature by methanol is calculated from

$$\Delta T = -\frac{RT_m^2}{\Delta H^{fus}(T_m)} \ln(1 - x_{MeOH}) \quad (25)$$

TABLE 2

Lattice and thermodynamic properties used in this study

		sI		sII		sH		
Average cell radius, R_m (Å)		3.95	4.30	3.91	4.73	3.91	4.06	5.71
Coordination number, z		20	24	20	28	20	20	36
H ₂ O molecules per unit cell		46		136		34		
Cavities per unit cell		2	6	16	8	3	2	1
$\Delta\mu_w^{(\beta-L \text{ or } \alpha,0)}$	J · mol ⁻¹	1263.60		883.82		1187.50		
$\Delta H_w^{(\beta-\alpha)}(T_0, p_0)$	J · mol ⁻¹	1389.08		1025.08		846.57		
$\Delta H_w^{(\alpha-L)}(T_0, p_0)$	J · mol ⁻¹	-6009.5						
$\Delta C_p^{(\beta-L)}$	$T \geq T_0$	J · mol ⁻¹ · K ⁻¹		-38.12				
$\Delta b^{(\beta-L)}(T_0)$		J · mol ⁻¹ · K ⁻²		0.141				
$\Delta C_p^{(\beta-\alpha)}(T_0)$	$T < T_0$	J · mol ⁻¹ · K ⁻¹		0.565				
$\Delta b^{(\beta-\alpha)}$		J · mol ⁻¹ · K ⁻²		0.002				

TABLE 3

Coefficients to calculate the fugacity of the empty hydrate

Coefficient × 10 ⁶	sI	sII	$I_{i,0}$	$I_{i,1}$
a_1	-112.2364	-111.3305	1	2
a_2	13.7154	12.5241	0	3
a_3	-10443.5035	-9765.9689	0	2
a_4	2725049.9757	2619579.9389	0	1
a_5	59305.0641	59967.2289	1	1
a_6	452.5014	313.3178	2	1
a_7	-237589591.4157	-235909838.5132	0	0
a_8	-7962184.1570	-7749197.5651	1	0
a_9	-113972.4068	-166339.7300	2	0
a_{10}	-726.6272	3841.3551	3	0

The model is verified with experimental data. For three-phase equilibria, it has an absolute average deviation in pressure of 8.86% ($N_p = 1396$). For two-phase equilibria, the absolute average deviation in water content is 6.07% ($N_p = 63$) and for systems inhibited with methanol the absolute average deviation in temperature is 1.04% ($N_p = 352$). The data is taken from (Sloan Jr., 1998; Morita et al., 2000; Holder & Hand, 1982; Ostergaard et al., 2000; Subramanian et al., 2000; Parrish & Prausnitz, 1972; Bishnoi & Dholabhai Pankaj, 1999) and more details of the hydrate model can be found in Osiaacz et. al. (2009).

5. Objective function

The network can be represented by graph $\mathbf{G} = (N, L, C)$ where $i \in N$ is a node, $j \in L$ is a pipe and $k \in C$ is a compressor unit. The node-pipe incidence matrix $\mathbf{A}_L = [a_{ij}^L]_{N \times L}$ has elements

$$a_{ij}^L = \begin{cases} 1, & \text{if pipe } j \text{ leaves node } i \\ -1, & \text{if pipe } j \text{ enters node } i \\ 0, & \text{otherwise} \end{cases} \quad (26)$$

and for the node-station incidence matrix, $\mathbf{A}_M = [a_{ik}^C]_{N \times C}$ the elements

$$a_{ik}^C = \begin{cases} 1, & \text{if node } i \text{ is the discharge node of station } k \\ -1, & \text{if node } i \text{ is the suction node of station } k \\ 0, & \text{otherwise} \end{cases} \quad (27)$$

and $\mathbf{A} = (\mathbf{A}_L, \mathbf{A}_M)$ is a $N \times (L + C)$ matrix. The mass flow rate through the pipe as vector is denoted as $\dot{\mathbf{m}} = (\dot{m}_1, \dots, \dot{m}_L)^\top$ and for the compressor driver as $\dot{\mathbf{n}} = (\dot{n}_1, \dots, \dot{n}_M)^\top$, with $\dot{\mathbf{u}} = (\dot{\mathbf{m}}^\top, \dot{\mathbf{n}}^\top)^\top$. The pressure vector is $\mathbf{p} = (p_1, \dots, p_N)^\top$ where p_i is the pressure at node i . The pressure bounds at each node are specified as \mathbf{p}^{\min} , \mathbf{p}^{\max} and the source vector as $\mathbf{s} = (s_1, \dots, s_N)^\top$ where s_i is the source at node i and in case of supply positive and delivery negative. The sum of sending and receiving at node i is zero, $\sum_i s_i = 0$. The network flow equations are described by

$$\begin{aligned} \mathbf{A}\dot{\mathbf{u}} &= \mathbf{s} \\ \mathbf{A}_L^\top \mathbf{p}^2 &= \phi(\dot{\mathbf{m}}) \end{aligned} \quad (28)$$

where $\mathbf{p}^2 = (p_1^2, \dots, p_N^2)^\top$ and $\phi(\dot{\mathbf{m}}) = [\phi_1(\dot{m}_1), \dots, \phi_L(\dot{m}_L)]^\top$.

In the latter expression, $\phi_1(\dot{m}_1) = c_j \dot{m}_j |\dot{m}_j|$, since Eq. can be formulated as

$$p_1^2 - p_2^2 = c_j \dot{m}_j |\dot{m}_j| \quad (29)$$

where p_1 and p_2 are the up- and downstream pressure of the pipe at the end nodes with \dot{m} as the mass flow rate through the pipe, respectively and c_j is given by

$$c_j = \frac{4^2 p_n z T}{\pi^2 z_n T_n \rho_n} \frac{fL}{d^5} \quad (30)$$

c_j are parameters describing the resistance of the specific pipe. The objective function is stated as follows

$$\begin{aligned}
 \min f(\dot{\mathbf{u}}, \mathbf{p}) &= \sum_{k=1}^m \dot{n}_k \\
 &\text{subject to} \\
 A\dot{\mathbf{u}} &= \mathbf{s}, \\
 \mathbf{B}_l \phi(\dot{\mathbf{m}}) &= 0, \\
 \mathbf{A}_l^\top \mathbf{p}^2 &= \phi(\dot{\mathbf{m}}), \\
 \mathbf{p} &\in [\mathbf{p}^{\min}, \mathbf{p}^{\max}], \\
 (p_{k,s}, T_{k,s}) &\in H \\
 (\dot{n}_k, p_{k,s}, p_{k,d}) &\in D_k, \quad k = 1, 2, \dots, m
 \end{aligned} \tag{31}$$

where B is the cycle matrix. The mass flow rate, surge pressure, temperature and discharge pressure at compressor station k are denoted as \dot{n}_k , $p_{k,s}$, $T_{k,s}$ and $p_{k,d}$, respectively. The feasible domain of compressor k is defined as D_k . To avoid hydrates, $p_{k,s}$ and $T_{k,s}$ must operate within in the hydrate free region H in which $p_{k,s} \leq p_H$ and $T_{k,s} \geq T_H$. Since the test network is acyclic, the constraint $B_l \phi(\dot{\mathbf{m}}) = 0$ is not applicable.

6. Case study

For both examples, the following assumptions are made (i) each station consist of two compressor units, which are identical and parallel installed, (ii) monotonicity of the p, T profiles and (iii) all compressors are operational. The following different pipeline configurations are investigated:

- i. *After cooling.* The compressed gas is cooled if $t_d > 30^\circ\text{C}$.
- ii. *No cooling.* The compressed gas is not cooled.
- iii. *Line heating.* A heater is installed directly after each compressor station, to avoid that the gas enters downstream the hydrate formation region.

The coefficients in Eqs. (7) and (8), defining the compressor envelope, are $c_1 = 7.7966 \times 10^{-5}$, $c_2 = 0.0916$, $c_3 = -82.650$, $c_4 = -0.9239$, $c_5 = 3.7652 \times 10^3$ and $c_6 = -1.9727 \times 10^6$. The margin for both surge and choke is set to 15% and $p_{s,\min} = 5.65$ MPa and $p_{d,\max} = 8.40$ MPa. The turbine efficiency as function of load for the turbines installed is

$$\eta_g = 0.0827 \cdot \ln(N_p) - 1.0644 \tag{32}$$

with N_p in W. The efficiency of the gas turbines is based on the units installed at the Yamal pipeline. These are driven by an ABB GT10 gas turbine with a power output of 24.6 MW, efficiency of 34.2% and 7700 rpm at nominal point.

Test network 1

The structure of the test network is illustrated in Fig. 3. The initial parameters (I) and (II) are based on reported values at the Yamal pipeline in Poland.

- (I) $S_2 = 0.203 \times 10^6 \text{ Nm}^3/\text{h}$, $S_3 = 0.15 \times 10^6 \text{ Nm}^3/\text{h}$, $S_4 = 2.33 \times 10^6 \text{ Nm}^3/\text{h}$, $p_{s,A} = 5.70 \text{ MPa}$, $t_{s,A} = 12.3 \text{ }^\circ\text{C}$ and $t_{soil} = 3.9^\circ\text{C}$.
- (II) $S_2 = 0.179 \times 10^6 \text{ Nm}^3/\text{h}$, $S_3 = 0.15 \times 10^6 \text{ Nm}^3/\text{h}$, $S_4 = 2.49 \times 10^6 \text{ Nm}^3/\text{h}$, $p_{s,A} = 5.90 \text{ MPa}$, $t_{s,A} = 11.9 \text{ }^\circ\text{C}$ and $t_{soil} = 3.1 \text{ }^\circ\text{C}$.

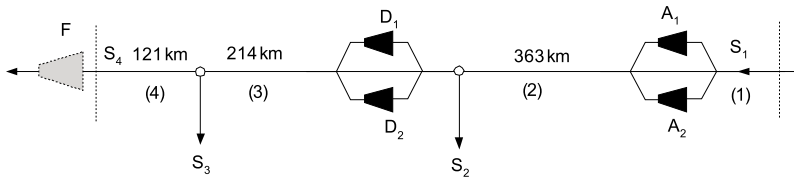


Fig. 3. Structure of the Yamal pipeline on Polish territory

The properties of the pipe wall are listed in Table 4. The soil conductivity is $2.05 \text{ W/m}\cdot\text{K}$. The total fuel consumption is presented in Table 5. By taking *after cooling* as reference situation, the fuel consumption for *no cooling* and *line heating* rises by 0.37% and 1.27% (I), respectively. For initial conditions (II), the corresponding values are 0.40% and 1.54%. Although, the difference between the scenarios seems marginal, the differences in annual fuel costs are substantial. The optimal settings for each hydrate combating method are presented in Table 6. Line heating, requires a significant increase in gas temperature. After cooling has a positive effect on the compressor power but the gas must be injected with methanol or dehydrated. The configuration *no cooling* requires less methanol and allows more dissolved water in the gas mainly due to the higher surge temperature at both sections. The working points for each compressor unit in case of line heating are presented in Fig. 5.

TABLE 4

Properties of pipe wall

Pipe wall structure	Thickness (mm)	k (W/m·K)
Internal coating	0.5	0.52
Steel L480MB (X 70)	19.22	45.3
External coating (polyethylene)	3.0	0.4

TABLE 5

Total fuel consumption of the compressor stations

Initial conditions	(I)			(II)		
	After cooling	No cooling	After heating	After cooling	No cooling	After heating
Fuel consumption ($\times 10^3 \text{ Nm}^3/\text{d}$)	408.3	409.8	413.5	420.9	422.6	427.4

TABLE 6

Optimized settings to avoid hydrates

Method	Station / section	(I)	(II)	
Line heating, $t_{heater, out}$ (°C)	Station A	63.4 ($\Delta t = 16.6$ °C) ^(a)	65.6 ($\Delta t = 19.1$ °C)	
	Station D	60.8 ($\Delta t = 32.0$ °C)	59.5 ($\Delta t = 30.8$ °C)	
Dehydration, x_w (ppmv)	Section A-D	After cooling	191.8	177.6
		No cooling	219.7	205.8
	Section D-F	After cooling	198.9	191.1
		No cooling	201.3	194.0
Methanol inhibition, x_M (wt%)	Section A-D	After cooling	5.47	6.52
		No cooling	2.76	3.58
	Section D-F	After cooling	5.61	6.40
		No cooling	5.38	6.10

(a) Δt is the difference between the outlet temperature of the heater and discharge temperature.

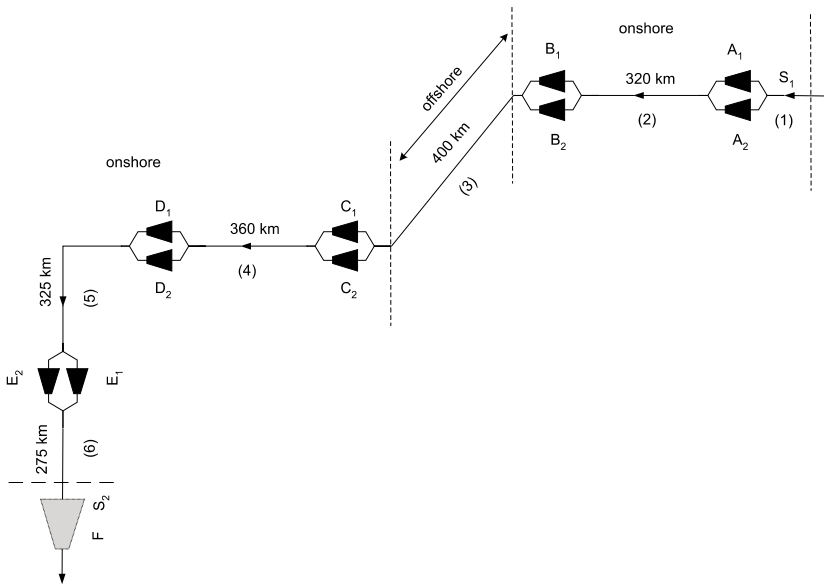


Fig. 4. Structure of the partial onshore and offshore transmission pipeline

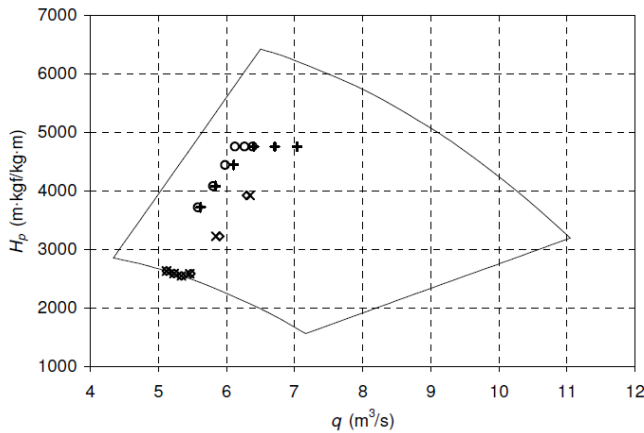


Fig. 5. Compressor envelope and working points for each compressor unit. Configuration is line heating.
 (+) Unit A₁, (o) A₂, (x) D₁ and (◊) D₂

Test network 2

This arbitrary selected example is a combination of a buried and deep-sea gas pipeline (Fig. 4). It consists five compressor stations with each two parallel units installed. The pipeline specifications and soil conductivity for the onshore sections are the same as in the previous example. For the offshore section, the total heat transfer is $1.8 \text{ W/m}^2 \cdot \text{K}$. At station A, $p_s = 5.70 \text{ MPa}$ and $t_s = 12.3^\circ\text{C}$. The soil and sea floor temperature are 3.9°C and 2.0°C , respectively. The total fuel consumption for different gas demands is presented in Table 7. By heating the compressed gas, the fuel cost of the stations rise between 1.54-3.10% compared with cooling. The corresponding range for no cooling is 0.20-0.61%. The parameters for each hydrate strategy as function of gas demand S_2 are presented in Figs. 6-8 whereas the water content and methanol concentration are calculated from the surge pressure and temperature. In Figure 7, the allowable water content at section E-F is increasing because the surge pressure at station F is equal to the minimum pressure (5.65 MPa). At increasing temperature with constant pressure, the water vapour content at which hydrates are stable is increasing. The increase at $2.7 \times 10^6 \text{ Nm}^3/\text{h}$ at section B-C is caused by the maximum discharge pressure (8.4 MPa) at station B. The amount of methanol required to prevent hydrates is presented in Figure 8. The working points for each compressor unit in case of line heating are presented in Fig. 9. The working points of the second compressor at each station is omitted in the graph because its operating point is the same.

TABLE 7

Total fuel consumption of the compressor stations

	Scenario	Demand S_2 ($\times 10^6 \text{ Nm}^3/\text{h}$)			
		2.4	2.5	2.6	2.7
Total fuel consumption all five stations ($\times 10^3 \text{ Nm}^3/\text{d}$)	After cooling	857.5	901.7	948.8	1008.7
	No cooling	859.2	904.2	953.6	1014.9
	Line heating	870.7	916.6	969.7	1040.0

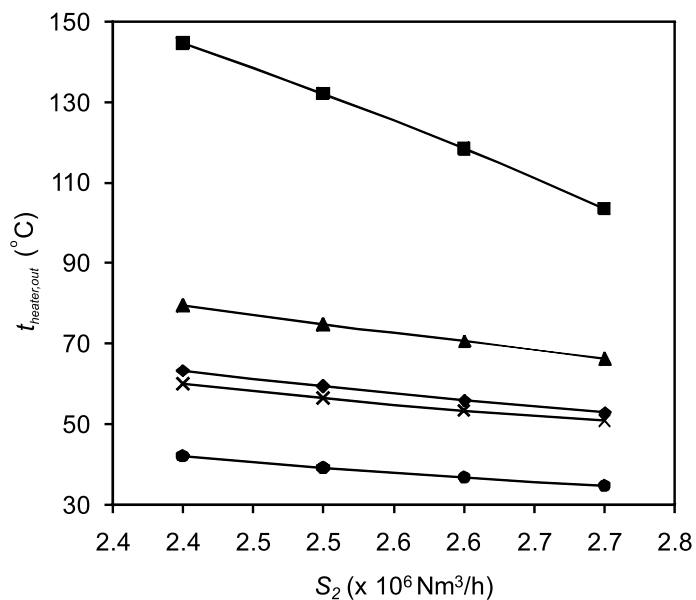


Fig. 6. Outlet gas temperature as function of demand S_2 .
 (—◆—) Station A, (—■—) station B, (—▲—) station C, (—×—) station D, (—●—) station E

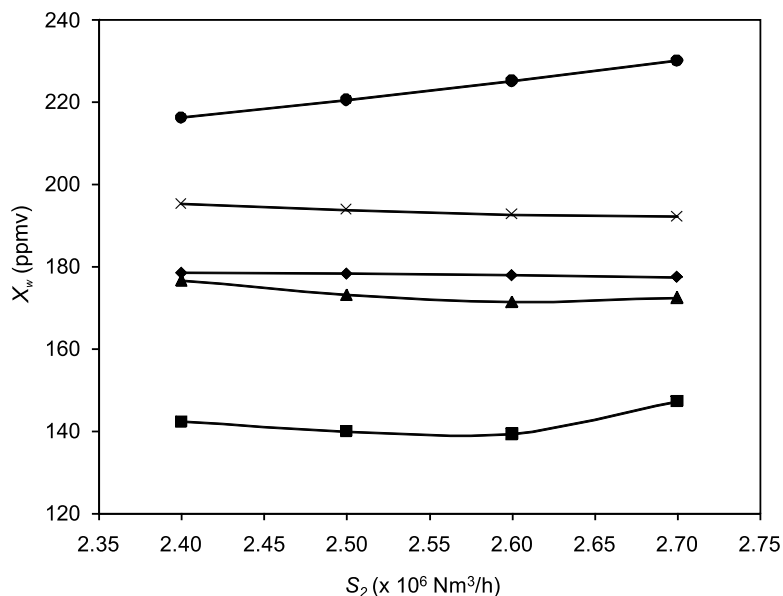


Fig. 7. Allowable water content as function of demand S_2 for the scenario after cooling.
 (—◆—) section A-B, (—■—) section B-C, (—▲—) section C-D, (—×—) section D-E, (—●—) section E-F

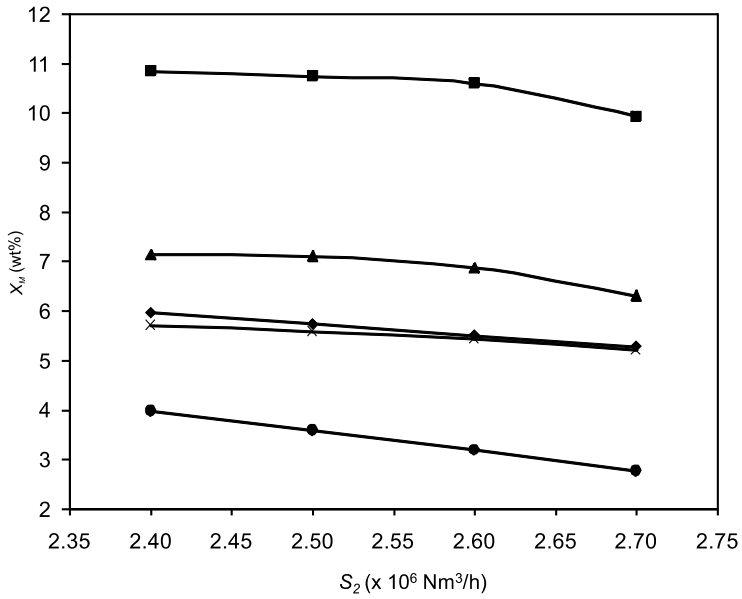


Fig. 8. Methanol concentration as function of demand S_2 for the scenario after cooling. (—◆—) section A-B, (—■—) section B-C, (—▲—) section C-D, (—×—) section D-E, (—●—) section E-F

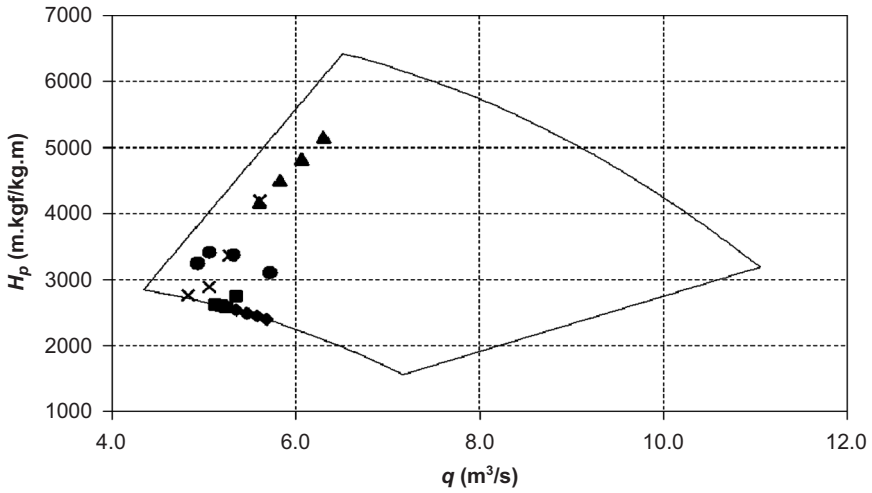


Fig. 9. Compressor envelope and working points for each compressor unit. Configuration is line heating. (▲) Unit A, (●) B, (×) C, (■) D and (◆) E

7. Conclusion

In this article the compressor fuel consumption is minimized subject to demand and hydrate prevention. This is achieved by calculating the compressor pressures and hydrate combating parameters, i.e., water vapour content in natural gas, methanol concentration and outlet temperature of the heater for each section of the pipeline. The mathematical structure of the compressors, network topology and pipe flow has been formulated.

The simulations for both test networks showed that after cooling results in the lowest compressor fuel costs. However, to preclude hydrates less water vapour is allowed in the gas or more volumes of methanol must be inhibited compared with no cooling. The fuel consumption decreases, though the costs of combating hydrates increase. Installing a line heater immediately after each station leads to a significant increase in fuel costs and considering the additional cost of running the heaters, this method is less feasible, especially for long-distance pipelines.

References

- Bishnoi P.R., Dholabhai Pankaj D., 1999. *Equilibrium conditions for hydrate formation for a ternary mixture of methane, propane and carbon dioxide, and a natural gas mixture in the presence of electrolytes and methanol*. Fluid Phase Equilibria, 158-160: p. 821-827.
- Hansen H.K., Rasmussen P., Fredenslund Aa., Schiller M., Gmehling J., 1991. *Vapor-Liquid Equilibria by UNIFAC Group Contribution*. 5. Revision and Extension. Ind. Eng. Chem. Res., 30: p. 2352-2355.
- Holder G.D., Hand J.H., 1982. *Multiple-Phase Equilibria in Hydrates from Methane, Ethane, Propane and Water Mixtures*. AIChE J., 28(3): p. 440-447.
- Holderbaum T., Gmehling J., 1991. *PSRK: A Group-Contribution Equation of State Based on UNIFAC*. Fluid Phase Equilibria, 70: p. 251-265.
- Klauda J.B., Sandler S.I., 2000. *A Fugacity Model for Gas Hydrate Phase Equilibria*. Ind. Eng. Chem. Res., 39: p. 3377-3386.
- Kreith F., Bohn M.S., 1993. *Principles of heat transfer*. 5th ed.
- Krichevsky I.R., Kasarnovsky J.S., 1935. *Thermodynamical calculations of solubilities of nitrogen and hydrogen in water at high pressures*. J. Amer. Chem. Soc., 57: p. 2168-2172.
- Morita K., Nakano S., Ohgaki K., 2000. *Structure and stability of ethane hydrate crystal*. Fluid Phase Equilibria, 169(2): p. 167-175.
- Osiadacz A., Uilhoorn F.E., Chaczykowski M., 2009. *Computation of Hydrate Phase Equilibria and Its Application to the Yamal-Europe Gas Pipeline*. Petroleum Science and Technology, 27(2) : 208-225.
- Ostergaard K.K., Tohidi B., Danesh A., Burgass R.W., Todd A.C., 2000. *Equilibrium data and thermodynamic modelling of isopentane and 2,2-dimethylpentane hydrates*. Fluid Phase Equilibria, 169: p. 101-115.
- Parrish W.R., Prausnitz J.M., 1972. *Dissociation Pressure of Gas Hydrates Formed by Gas Mixtures*. Ind. Eng. Chem. Process Des. Develop., 11(1): p. 26-35.
- Sloan Jr., E.D., 1998. *Clathrate hydrates of natural gases*. 2 ed., New York: Marcel Dekker Inc.
- Soave G., 1972. *Equilibrium constants from a modified Redlich-Kwong equation of state*. Chem. Eng. Sci., 27: p. 1197-1203.
- Subramanian S., Kini R., Dec S.F., Sloan Jr., E.D., 2000. *Evidence of structure II hydrate formation from methane + ethane mixtures*. Chem. Eng. Sci., 55(11): p. 1981-1999.
- Techo R., Tickner R.R., James R.E., 1965. *An accurate equation for the computation of the friction factor for smooth pipes from the Reynolds number*. Journal of Applied Mechanics, p. 443.
- Van der Waals J.H., Platteeuw J.C., 1959. *Clathrate Solutions*. Adv. Chem. Phys., 1: p. 1-57.
- Yoon J.-H., Yoshitaka Y., 2004. *PSRK Method for Gas Hydrate Equilibria: I. Simple and Mixed Hydrates*. AIChE Journal, 50(1): p. 203-214.